


Article

Potential Roles of Three ABCB Genes in Quinclorac Resistance Identified in *Echinochloa crus-galli* var. *zelayensis*

Yuanlin Qi ^{1,2} , Yongli Guo ^{1,2}, Xudong Liu ^{1,2}, Yuan Gao ^{1,2}, Yu Sun ^{1,2}, Liyao Dong ^{1,2} and Jun Li ^{1,2,*}¹ College of Plant Protection, Nanjing Agricultural University, Nanjing 210095, China² Key Laboratory of Integrated Management of Crop Diseases and Pests (Ministry of Education), Nanjing Agricultural University, Nanjing 210095, China

* Correspondence: li_jun@njau.edu.cn

Abstract: *Echinochloa crus-galli* var. *zelayensis* is a variant of *E. crus-galli* (L) Beauv, and it is the most pernicious weed in the east of China. Quinclorac, as synthetic auxin herbicide, could control this kind of weed effectively. In this study, two populations were used to further research the mechanism of quinclorac resistance, and the *EcABCB1*, *EcABCB4* and *EcABCB19* was functionally characterized to determine their roles in quinclorac resistance. It was found that root growth of quinclorac-resistant biotype SSXB-R was less inhibited by quinclorac at 5 μ M and 50 μ M when compared with the susceptible biotype JNNX-S. The results show that the IAA variations in root tip of JNNX-S were significantly higher than SSXB-R at 12 h after treatment with quinclorac (50 μ M) and 1-N-naphthylthalamic acid (100 μ M). There are no significant differences in IAA variations of the basal part of the root between susceptible and resistant biotypes after treatment with quinclorac and 1-N-naphthylthalamic acid (NPA). The transcript level of *EcABCB1* and *EcABCB19* in the root of JNNX-S showed down-regulated and up-regulated after treatment with quinclorac (TWQ) at 6 h in susceptible and resistant biotypes compared with control, respectively. The transcript level for *EcABCB4* in the root showed up-regulated after TWQ at 12 h only in susceptible biotypes compared with control. It was found that the IC₅₀ to quinclorac of *AtABCB4* and *AtABCB19* mutants were significantly higher than the parent line Col-0.

Keywords: ABCB transporter; *Echinochloa crus-galli* var. *zelayensis*; quinclorac resistance

Citation: Qi, Y.; Guo, Y.; Liu, X.; Gao, Y.; Sun, Y.; Dong, L.; Li, J. Potential Roles of Three ABCB Genes in Quinclorac Resistance Identified in *Echinochloa crus-galli* var. *zelayensis*. *Agronomy* **2022**, *12*, 1961. <https://doi.org/10.3390/agronomy12081961>

Academic Editor: Ilias Travlos

Received: 16 July 2022

Accepted: 18 August 2022

Published: 19 August 2022

Publisher's Note: MDPI stays neutral with regard to jurisdictional claims in published maps and institutional affiliations.



Copyright: © 2022 by the authors. Licensee MDPI, Basel, Switzerland. This article is an open access article distributed under the terms and conditions of the Creative Commons Attribution (CC BY) license (<https://creativecommons.org/licenses/by/4.0/>).

1. Introduction

E. crus-galli var. *zelayensis* is one of the most troublesome weeds of rice fields in China [1]. Quinclorac, which belongs to quinolinecarboxylic acid, is one of the auxin herbicides [2,3]. Quinclorac resistance mechanism is closely related to ethylene. In susceptible *E. crus-galli* var. *zelayensis*, ethylene production showed increased trends within 12 h after treatment with quinclorac, and the ethylene production in the resistant population was not significantly changed after treatment with quinclorac [4]. Accumulation of ethylene could inhibit photosynthesis; subsequently, reactive oxygen species and H₂O₂ could be produced and finally lead to plant death [5,6]. The association between auxin and ethylene at the physiological and molecular level has been reported. It is reported that ethylene is not required for the auxin-induced growth inhibition in either roots or hypocotyls of dark-grown seedlings. On the contrary, auxin seems to be indispensable for growth inhibition in roots induced by ethylene [7]. Ethylene can travel through the plant by diffusion; Indole-3-acetic acid (IAA) is transported by a complex net of carriers, such as ABC transporters [8].

In the past decades, it has been reported that auxin could be transported by a group of ATP binding cassette (ABC) transporters which belong to the multidrug resistance (MDR)-like family, also known as the P-glycoproteins (PGPs) [9,10]. ABCBs are the second largest ABC protein subfamily in plants. There is a growing understanding about the importance of ABCB transporters in plants as more ABCB transporters have been well characterized

in non-plant eukaryotic systems [11]. There are plant ABCBs linked specifically to auxin efflux and to physiological responses dependent on their correct function [12]. ABCB1 and ABCB19 are located in the *Arabidopsis thaliana* plasma membrane (PM). They can bind the auxin efflux inhibitor 1-N-naphthylthalamic acid (NPA) with high affinity [13–17]. Loss of ABCB19 and ABCB1 function results in reduced auxin transport in *Arabidopsis thaliana* [13]. Furthermore, increasing auxin efflux were found in yeast of heterologous expression of ABCB1 [18]. At low auxin concentrations, AtABCB4 functions as auxin uptake; however, at high auxin concentrations, it functions as auxin export [19]. Although the sequence similarity is 60% and 61%, respectively, comparing AtABCB4 with AtABCB1 and AtABCB19, the results of the transport assay of AtABCB4 in HeLa cells and yeast are contrary to those of AtABCB1 and AtABCB19 [20]. These results indicate that the complementary expression patterns of AtABCB4 and AtABCB19 are consistent with their complementary functions [20].

ABCBs take part in many stress responses, and their expression could be suppressed or induced by stresses. For example, many members of ABC transporter play a role in the process of xenobiotic detoxification, polar auxin transport and disease resistance [10,21–27]. Some small molecule drugs were regarded as substrates of ABCB transporters, and resistance to small molecule drugs may be due to the alteration of ABCB abundance in plasma membrane [28]. A better understanding of this family of plant transport proteins is relevant to avoiding synthetic auxin herbicide (SAH) resistance evolution. Moreover, 4D resistance is associated with ABCB transporter activity, although impaired long-distance transport and not increased cellular efflux, which consequently reduced accumulation inside cells, appeared to be the basis of resistance [29]. Meanwhile, up-regulation of an efflux carrier would likely accelerate extrusion of substrate auxins from cells, which may confer resistance by removing herbicide [30]. ABCB transporter seems to play an important role in auxinic herbicide resistance.

2. Materials and Methods

2.1. Plant Material

The *E. crus-galli* var. *zelayensis* seeds were collected from paddy fields in Nanjing, Jiangsu Province (32.04° N, 118.8° E) and Shanghai (30.94° N, 121.07° E), in China. The seeds of two biotypes were sown in pots containing a 1:1 (wt/wt) mixture of sand and soil (pH = 5.6). All pots were placed on the growth chamber in growing season. Half seedlings of two biotypes were treated by quinclorac (recommended dose 300 g AI ha⁻¹) at 2.5–3.5 leaves stage. The survival was recorded after three weeks treatment. Seeds were collected from surviving plants and regarded as a resistant population (SSXB-R; ED₅₀ value 2457.79 g·ha⁻¹). Seeds of the susceptible population (JNNX-S; ED₅₀ value 36.75 g·ha⁻¹) were collected from plants not treated with quinclorac [1]. Two populations, JNNX-S and SSXB-R, were used in this study.

2.1.1. Effects of Quinclorac and NPA on Root Growth of Two Populations

Root assays were performed on 13 × 13 cm square Petri dishes with 1/2 MS and 1.5% sucrose and 1% phytoagar. Quinclorac (analytical standard, PESTANAL®, Sigma-Aldrich, St. Louis, MO, USA) and NPA (Dixiai, Shanghai) were dissolved by dimethyl sulfoxide (DMSO) to 1 mM. Stock solutions of quinclorac were diluted into 0.5 μM, 5 μM and 50 μM in the medium. Stock solutions of NPA were diluted into 1 μM, 10 μM and 100 μM in the medium. The DMSO (50 μM) was used as control. The seeds of two biotypes were surface-sterilized (8% NaClO) and then washed by double distilled water (dd H₂O). The seeds were planted in medium without quinclorac and moved to a growth chamber for 7 days (12/12 h light/dark photoperiod, 30 °C/25 °C, light intensity 300 μmol m⁻² s⁻¹), and then seedlings (10 seedlings per petri dish) were transferred to medium with quinclorac alone (0 μM, 0.5 μM, 5 μM and 50 μM) and NPA alone (0 μM, 1 μM, 10 μM and 100 μM) for 7 days for determination of root length.

2.1.2. Effects of Quinclorac and NPA on IAA Contents in Roots of Two Populations

Seeds of two biotypes were pre-germinated in a petri dish filled with water. The germinated seeds were transplanted to disposable cups containing 300 mL Kasugai nutrient solution in a growth chamber at 30/25 °C with 12 h of light (300 $\mu\text{mol m}^{-2} \text{s}^{-1}$) and 12 h of darkness per day. Quinclorac (analytical standard, PESTANAL[®], Sigma-Aldich, St. Louis, MO, USA) and NPA were dissolved in DMSO to the concentration of 0.1 mol/L. A stock solution of quinclorac and NPA were added to Kasugai nutrient solution to a final concentration of 50 $\mu\text{mol/L}$ [31] when the plants grew at 2.5–3 leaf stage and then placed back in the growth chamber at 30 °C day/25 °C night under the 12 h/12 h photoperiod with light intensity (300 $\mu\text{mol m}^{-2} \text{s}^{-1}$). The root was divided in two parts. One is a root tip (from root tip 0.5 cm), and another is the upper root tissue (from root basis 0.5 cm). The root tips (0.2 g) and upper root tissues (0.2 g) were used for determination of IAA contents after TWQ at 6 h, 12 h and 24 h. Root tips and upper root tissues without treatment with quinclorac were regarded as control. The IAA contents were determined by enzyme-linked immunosorbent assay (ELISA). Each treatment included three replicates.

Sample powders were transferred into a tube containing 1.2 mL phosphate buffer saline (PBS) and then incubated at 4 °C for 4 h. The extracting solution was then centrifuged at 10000 g/min for 10 min at 4 °C, and supernatants were transferred to a new tube. PBS (1 mL) was added to the sediment, followed by vortex to resuspend the extracts. The tubes were then incubated at 4 °C for another 1 h and re-centrifuged. Supernatant from the two centrifuging were pooled and weighted. IAA in the supernatant was extracted by a C-18 column. The extraction solution was transferred to a 2 mL centrifugal tube, and 200 μL of the solution was dried with nitrogen. IAA content was determined by enzyme-linked immunosorbent assay provided by China Agricultural University. Briefly, 0.2 mL optimal coating concentration of antibody in a carbonate buffer (PH 9.6) was added to each well, and the plate was incubated at 37 °C for two hours and washed three times with PBS-T (8.0 g NaCl, 0.2 g KH_2PO_4 , 2.96 g $\text{Na}_2\text{HPO}_4 \cdot 12\text{H}_2\text{O}$, Tween-20 0.5 mL, in 1000 mL water). Reference material (IAA) and sample were added to a 96-well ELISA plate, and then antibodies were added to each well. The plate was put in a humidified box under 37 °C for 0.5 h. The solution in the plate was discarded, and the plate was washed three times. Horseradish peroxidase (HRP-IgG) was added to each well, and the plate was put in a humidified box under 37 °C for 30 min. The solution was discarded, and the plate was washed three times. O-Phenylenediamine (OPD) substrate solution (0.2 mL, containing 4 mg OPD in 10 mL substrate buffer, pH 5.0, with the addition of 15 μL of 30% H_2O_2 before use) was freshly prepared. A substrate buffer (citric acid 0.467 g, $\text{Na}_2\text{HPO}_4 \cdot 12\text{H}_2\text{O}$ 1.843 g, dissolved in 100 mL sterilized ultrapure water) was added and incubated at 37 °C for 30 min. Then 50 μL of 2 M H_2SO_4 was added to stop the reaction. Finally, a substrate solution was added to each well and showed dark color. The enzyme activities were measured immediately at 490 nm.

The results of ELISA were calculated by Logit curve, and the formula is shown below.

$$\text{Logit}(B/B_0) = \ln B/B_0 - B \quad (1)$$

where B_0 is the value of 0 ng/mL well; and B is the value of other concentration.

2.2. Amplification of ABCB Family Genes

The seeds of two biotypes were planted in pots (47.5 mm \times 35.5 mm \times 30.5 mm) containing a 1:1 (wt/wt) mixture of sand and clay and 50% organic fertilizer. The pots were placed in a growth chamber at 30/25 °C with 12 h light (300 $\mu\text{mol m}^{-2} \text{s}^{-1}$) and 12 h darkness each day. The single plants were used for RNA extraction at the 2.5–3 leaf growth stage. Total RNA from the leaf of JNNX-S and SSXB-R were extracted using Transzol Up (Tiangen Biotech, Beijing, China) according to the manufacturer's protocol, and then the RNA samples were reverse-transcribed to cDNA using the PrimeScript RT Reagent Kit with gDNA Eraser (TaKaRa, Otsu, Japan). Primers (Table 1) were designed for amplification

of the partial ABCBs genes based on the ABCBs gene sequence of *Echinochloa crusgalli* (L.) Beauv. from its genome database (<https://www.ncbi.nlm.nih.gov/> (accessed on 1 July 2019)). The polymerase chain reaction (PCR) was conducted in 50 μ L volume, consisting of 1 μ L cDNA, 2 μ L of each primer (10 μ M), 25 μ L 2 \times Rapid Taq Master Mix (Vazyme Biotech Co., Ltd., Nanjing, China) and 20 μ L ddH₂O. Amplification was conducted as follows: 5 min at 95 $^{\circ}$ C for cDNA denaturation; 35 cycles of 30 s at 95 $^{\circ}$ C for cDNA denaturation, 30 s at X $^{\circ}$ C for annealing, Y s at 72 $^{\circ}$ C for DNA elongation and a final elongation of 10 min at 72 $^{\circ}$ C. (X and Y in the Table 1). The PCR products were purified and then cloned into the pMD19-T vector (TaKaRa Biotechnology, Dalian, China). Plasmids containing the fragment were sequenced. Sequences were aligned and compared using the BioEdit Sequence Alignment Editor (Tom Hall, Carlsbad, CA, USA). The sequences were aligned and compared using BioEdit Sequence Alignment Editor Software.

Table 1. The primer sequences for amplification of *EcABCBs* genes.

Gene	Primer Sequence (5'-3')	Temperature	Time
<i>EcABCB1</i>	TTGGTTGCCCTCCTIGTIG GCACTCATCTTTGTCGGTCT	60 $^{\circ}$ C	40 s
<i>EcABCB4-1</i>	ATGGCTGGCGAAAGGCAGTCAG TAAGCGCCACAACATCAAGAGGC	64.3 $^{\circ}$ C	2 min
<i>EcABCB4-2</i>	TCGACTACAAGAGACACGTGCTGATG GAGCGGAGCTCTATTAGTGAAGCG	62.9 $^{\circ}$ C	2 min
<i>EcABCB19</i>	TCACCTCCACGGACAATC TGCGCTCTACTTCGTCTACC	51.7 $^{\circ}$ C	1 min

2.3. ABCB Family Genes Expression

Plants were cultivated, treated with quinclorac under experimental conditions as described in the effects of quinclorac and NPA on IAA contents of root in *E. crus-galli* var. *zelayensis*. The roots of the plants were harvested after treatment with quinclorac at 0 h, 6 h, 12 h, 24 h and 48 h. The RNA extraction and cDNAs synthesis were conducted as described above. The *E. crus-galli* β -actin gene (Genbank accession number: HQ395760) was used as a candidate reference gene. Clonal sequences of ABCBs genes were used to design primers (Table 2) for qRT-PCR using <http://bioinfo.ut.ee/primer3-0.4.0/> (accessed on 1 May 2020); q-PCR analyses were performed on ABI-7500 Fast Real-Time PCR system (Applied Biosystems, Waltham, MA, USA) using SYBR qRT-PCR Master Mix (Vazyme Biotech Co., Ltd., Nanjing, China) following the protocols. The relative mRNA level was calculated by the $2^{-\Delta\Delta CT}$ method [4]. The experiment included three biological replicates and was repeated twice.

Table 2. Gene expression in *E. crus-galli* var. *zelayensis* was determined by qRT-PCR.

Gene	Primer Sequence (5'-3')
<i>EcABCB1</i>	F: GGGAAGAGCACCGTAGTGTC R: GCAGGTTCTCCTTGATGCTC
<i>EcABCB4</i>	F: TATAATGACGGGGCAATGT R: CTCTGGTCTTGCTGGGTAGCT
<i>EcABCB19</i>	F: TGCTAGGAGTTCGTCGTGTG R: GCTACCAGCGCTTTAGATGC

2.4. Susceptibility to Quinclorac in *Arabidopsis* T-DNA Insertional Mutants

The mutants and parent line (*col-0*) seeds were planted in pots (47.5 mm \times 35.5 mm \times 30.5 mm) containing a 50% vermiculite and 50% organic fertilizer. The pots were placed in a growth chamber at 22/22 $^{\circ}$ C with 16 h light (12,000 lx) and 8 h darkness each day. The single plants were used for DNA extraction after 10 days. Total DNA from leaves of mutants and the parent line were extracted using Transzol Up (Tiangen Biotech,

Beijing, China) according to the manufacturer's protocol. For identification of mutant lines carrying T-DNA insertions in the ABCBs genes, all ABCBs T-DNA insertion lines available through the Arabidopsis Information Resource (TAIR) and the parent line through our lab were screened using the gene-specific primers (Table 3). PCR was performed using these primers in combination with LBb1.3 (ATTTTGCCGATTTTCGGAAC). All of the primers were designed using <http://signal.salk.edu/tdnaprimers.2.html> (assessed on 1 June 2020). The polymerase chain reaction (PCR) was conducted in 10 µL volume, consisting of 0.2 µL DNA, 0.4 µL of each primer (10 µM), 5 µL 2 × Rapid Taq Master Mix (Vazyme Biotech Co., Ltd., Nanjing, China) and 4 µL ddH₂O. Amplification was conducted as follows: 5 min at 95 °C for DNA denaturation; 35 cycles of 30 s at 95 °C for DNA denaturation; 30 s at 60 °C for annealing; 30 s at 72 °C for DNA elongation and a final elongation of 10 min at 72 °C. We verified homozygous T-DNA insertional lines ABCB1 (SALK_066872), ABCB4 (SALK_067653) and ABCB19 (SALK_080316).

Table 3. Screening Arabidopsis T-DNA insertional mutants using specific primers.

Gene	Primer Sequence (5'-3')
ABCB1	LP: TTTTGGTCGAGTCTGATTGG
	RP: TCCTTGAACCAACCAACAAAG
	RP: CTTTCGTGACCTATGTTTCGC
ABCB4	LP: GATTAAGCCCAAGTTCGATCC
	RP: ATGGATTCATCAGTGGTCTGC
	LP: AGATCATAACATCAGGCCGTG
ABCB19	RP: TTTTGC AATTTGGTCCTGTC

To assess the susceptibility of mutants and the parent line to quinclorac, seeds of vernalization were grown vertically on 1/2 MS plates for 7 days, and then 10 seedlings were transferred to 1/2 MS (Control) and 1/2 MS+ quinclorac (1.3 µM, 3.7 µM, 11.1 µM, 33.3 µM, 100 µM, 300 µM) plates for 7 days. The root length was measured. For each treatment, at least 10 replicates were imaged and tested. The conditions of cultivation were described as screening the homozygous mutants.

2.5. Statistical Analysis

The IC₅₀ values, confidence interval, correlation coefficient and regression equation were calculated using DPS [32]. Sigma Plot (SigmaPlot Software Inc, Chicago, IL, USA) was used to draw the graphs. For comparison of differences in root length among two biotypes, mutants and the parent line, Duncan's Multiple Range Test ($p < 0.05$) was used, and ANOVA was conducted using SPSS 20 (SPSS, Chicago, IL, USA).

3. Results and Discussion

3.1. Effects of Quinclorac and NPA on Root Growth of Two Populations

As an auxin herbicide, quinclorac can cause symptoms of growth inhibition, epinasty and tissue decay in high concentrations [33]. In this study, the root growth in both a susceptible and a resistant population were inhibited by quinclorac. The root length of susceptible and resistant biotypes was significantly less than control after treatment with quinclorac (Figure 1). Root length in resistant biotypes was significantly higher than susceptible biotypes after TWQ (5 µM, 50 µM). Meanwhile, after treatment with NPA (100 µM), the root length of resistant and susceptible biotypes was significantly less than control (Figure 2). The root length of resistant biotypes was also significantly higher than susceptible biotypes after treatment with NPA at 10 µM.

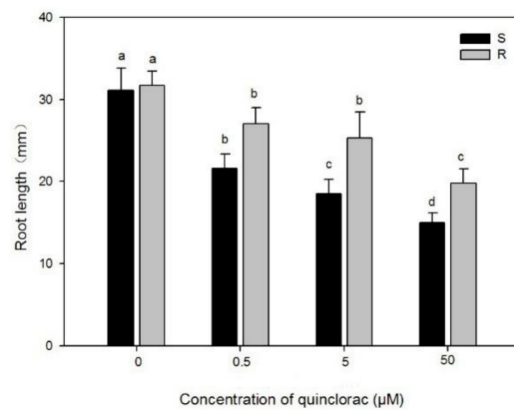


Figure 1. Root length of two biotypes at 7 days after treatment with 0 μM , 0.5 μM , 5 μM and 50 μM quinclorac. S represents the susceptible biotypes (JNNX-S), and R represents the resistant biotypes (SSXB-R). Data are the mean values of at least 10 biological replicates. The standard errors of the means are described by vertical bars. ANOVA significance groupings are shown as a, b and c.

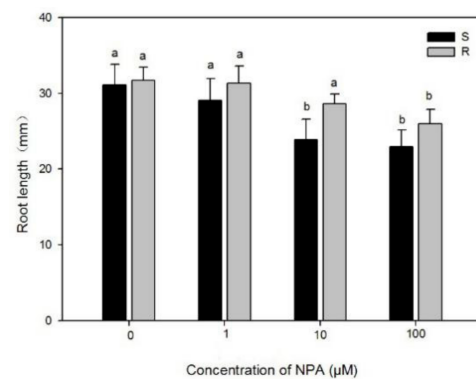


Figure 2. Root length of two biotypes at 7 days after treatment with 0 μM , 1 μM , 10 μM and 100 μM 1-N-naphthylthalamic acid (NPA). S represents the susceptible biotypes (JNNX-S), and R represents the resistant biotypes (SSXB-R). Data are the mean values of at least 10 biological replicates. The standard errors of the means are described by vertical bars. ANOVA significance groupings are shown as a and b.

3.2. Effects of Quinclorac and NPA on IAA Variation in Roots of Two Populations

Several studies have revealed that ethylene plays a pivotal role in the quinclorac resistance mechanism [1,34]. It has been proved that ethylene content of susceptible *Galium aparine* was three times higher compared with untreated controls; whereas the ethylene content hardly changed after treatment with quinclorac in quinclorac-resistant *G. aparine* [35]. Moreover, the amount of increasing ethylene in a susceptible biotype of *Digitaria ischaemum* was three times higher than that in a quinclorac-resistant biotype after quinclorac treatment [36]. Meanwhile, it has been proved that the ethylene biosynthesis can be induced by IAA [7]. However, no evidence has proved the relationship between IAA variation trends and ABCBs transporter after treatment with quinclorac which may involve the resistance mechanism of quinclorac in *E. crus-galli* var. *zelayensis*.

The IAA variation trends in root tips were affected by quinclorac in both susceptible and resistant biotypes. After treatment with quinclorac at 50 μM , IAA variation trends in root tips showed increased trends in susceptible and resistant biotypes from 0 h to 12 h, but the IAA variation trends of root tips in susceptible biotypes were significantly higher than resistant biotypes (Figure 3). The IAA variation trends of root tips were 4.12 times and 2.41 times compared with controls in susceptible and resistant biotypes after TWQ at 12 h, respectively. It is worth noting that the IAA variation trends in root tips were also affected by NPA and showed the same trends (Figure 4). After treatment with NPA at 100 μM , the IAA variation trends in root tips were 3.43 times and 2.35 times compared

with controls in susceptible and resistant biotypes at 12 h, respectively. IAA variation trends in root tips of susceptible biotypes were also significantly higher than the resistant biotypes after treatment with NPA. In addition, the IAA variation in upper root tissue was also determined. IAA variation in upper root tissue of resistant biotypes was higher than susceptible biotypes after treatment with quinclorac (50 μ M) at 6 h. However, there were no significant differences between susceptible and resistant biotypes in IAA variation trends after treatment with quinclorac at 50 μ M (Figure 5) and NPA 100 μ M (Figure 6).

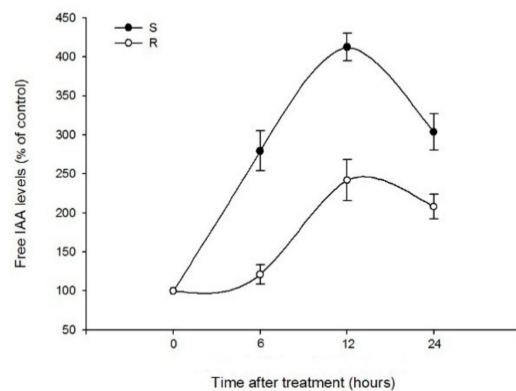


Figure 3. IAA contents in root tips were measured in S (JNNX-S) and R biotypes (SSXB-R) after treatment with quinclorac (50 μ M) at 0 h, 6 h, 12 h and 24 h. Data are the mean values of at least three biological replicates. The standard errors of the means are described by vertical bars.

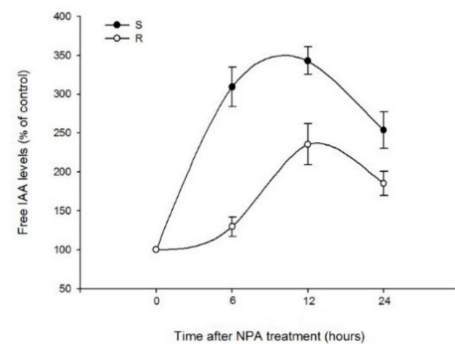


Figure 4. IAA contents in root tips were measured in S (susceptible, JNNX-S) and R biotypes (resistant, SSXB-R) after treatment with 1-N-naphthylthalamic acid (NPA) (100 μ M) at 0 h, 6 h, 12 h and 24 h. Data are the mean values of at least three biological replicates. The standard errors of the means are described by vertical bars.

3.3. Sequencing and Expression of ABCBs Genes

Many aspects of auxin action depend on its distribution within plant tissues [11]. In addition to local biosynthesis and the release of active forms from inactive precursors, the auxin distribution depends on its directional transport. ABCB proteins function in phytohormone auxin transport. The AtABCB1 and AtABCB19 were identified and associated with auxin transport. The phenotypes suggest that the free IAA contents and basipetal auxin transport are severely reduced in AtABCB19 and AtABCB1 mutants [18]. AtABCB4 shows an auxin uptake activity at low auxin concentrations and, conversely, an export activity at high auxin concentration [19]. It is reported that AtABCB1, AtABCB4 and AtABCB19 proteins bind tightly and specifically to the auxin transport inhibitor 1-naphthylphthalamic acid (NPA) [14–17].

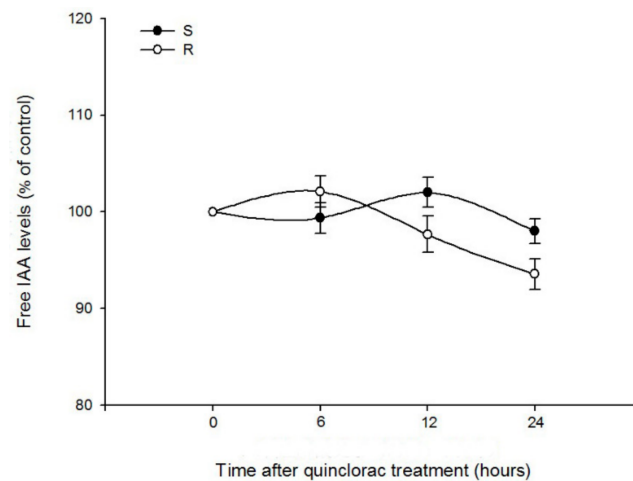


Figure 5. IAA contents in upper root tissues were measured in S (susceptible, JNNX-S) and R biotypes (resistant, SSXB-R) after treatment with quinclorac (50 μ M) at 0 h, 6 h, 12 h and 24 h. Data are the mean values of at least three biological replicates. The standard errors of the means are described by vertical bars.

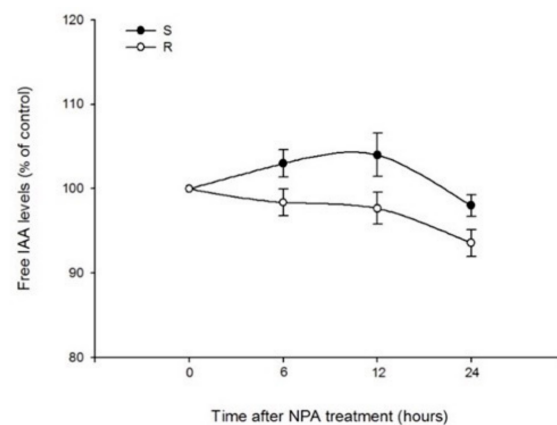


Figure 6. IAA contents in upper root tissues were measured in S (susceptible, JNNX-S) and R biotypes (resistant, SSXB-R) after treatment with 1-N-naphthylthalamic acid (NPA) (100 μ M) at 0 h, 6 h, 12 h and 24 h. Data are the mean values of at least three biological replicates. The standard errors of the means are described by vertical bars.

The partial sequence of *EcABCB1*, *EcABCB4* and *EcABCB19* was cloned, and the sequence was uploaded to the National Center for Biotechnology Information (NCBI) with accession numbers MH392229, MH392230 and MH392231. Some studies suggest that resistance to synthetic auxin herbicide (SAH) is likely to be conferred by a single, semi-dominant gene, but the number and the nature (i.e., transporters, receptors, signal transduction complexes) of the genes conferring auxin resistance is currently unknown. Yang has hypothesized that a single major gene may play a role for quinclorac resistance in *E. crus-pavonis* [37]. However, we do not find any mutations for *EcABCBs* genes in resistant *E. crusgalli* var. *zelayensis*.

It is undoubtedly true that auxin entering basal tissues in plants from the apical regions is transported through the central tissues of the root toward the tip [38]. However, ABCB family members have different auxin transport directionalities. Highly tissue specific expression and subcellular localization largely determine transport directionalities [20]. AtABCB1 is localized in all root cells [39], whereas AtABCB19 is restricted to the endodermis and the pericycle [40], and AtABCB4 is distributed in the epidermis and the lateral root cap. This localization pattern may contribute to the acropetal and basipetal auxin transport [20].

The complementary expression patterns of *AtABCB4* and *AtABCB19* fit well with their complementary functions (acropetal vs. basipetal auxin transport).

The ABCBs family genes expression levels in roots and leaves of JNNX-S and SSXB-R were compared. *EcABCB1* (Figure 7A) expression in roots showed up-regulated and down-regulated after treatment with quinclorac at 6 h compared with control in resistant and susceptible biotypes, respectively. The expression of *EcABCB1* showed down-regulated trends after quinclorac treatment at 12 h and 48 h compared with 6 h. *EcABCB4* expression in root showed up-regulated in susceptible biotypes only after TWQ at 6 h. The expression of *EcABCB4* (Figure 7B) reached the peak after quinclorac treatment at 12 h. *EcABCB19* (Figure 7C) expression in root showed up-regulated and down-regulated after treatment with quinclorac at 6 h compared with control in resistant and susceptible biotypes, respectively. The expression of *EcABCB19* showed down-regulated trends after quinclorac treatment at 12 h and 48 h compared with 6 h.

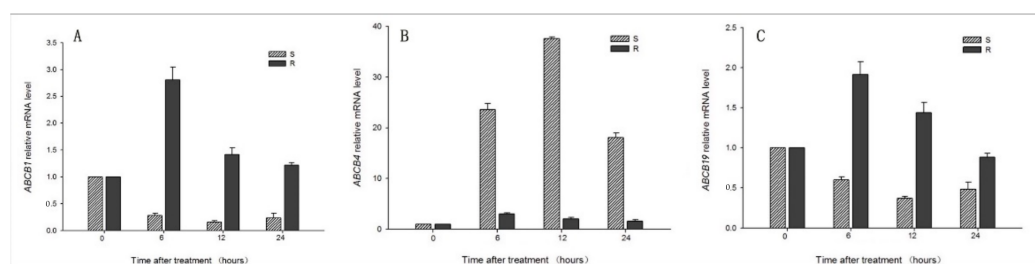


Figure 7. Relative transcript level in roots of 3 candidate genes after treatment with quinclorac in S (susceptible, JNNX-S) and R (resistant, SSXB-R) biotypes. (A–C) represent the *EcABCB1*, *EcABCB4* and *EcABCB19*.

3.4. Susceptibility to Quinclorac in ABCB Mutants of *A. thaliana*

To further determine the role of ABCBs/IAA regulation in quinclorac resistance, we measured the root growth after treatment with quinclorac at a series of concentrations in the parent line and ABCB T-DNA insertional mutations of *Arabidopsis*. There was no visual difference between the parent line and *AtABCB* mutations in the root system after treatment with quinclorac at 300 μM , and all the plants died. Both the parent line and *AtABCB* mutations showed phytotoxin symptoms, such as leaf withering and reduced root length, after quinclorac treatment in seven days at 100 μM . However, the root length showed inhibition after TWQ compared to without quinclorac treatment in the *AtABCB1* mutation (Figure 8A). In addition, the growth trends of root in *AtABCB4* and *AtABCB19* mutations (Figure 8B,C) showed the same trend as the *AtABCB1* mutation. It is worth noting that the root length of the plants having these mutations is shorter compared with the root length of the parent line after TWQ at 1.3, 3.7, 11.1 μM . The IC_{50} were 11.77 μM for the parent line. The *AtABCB1*, *AtABCB4* and *AtABCB19* mutant's IC_{50} were 10.61 μM , 49.91 μM and 44.03 μM (Table 4). Therefore, we speculate that *EcABCB4* and *EcABCB19* could be involved in quinclorac resistance via regulating IAA transportation.

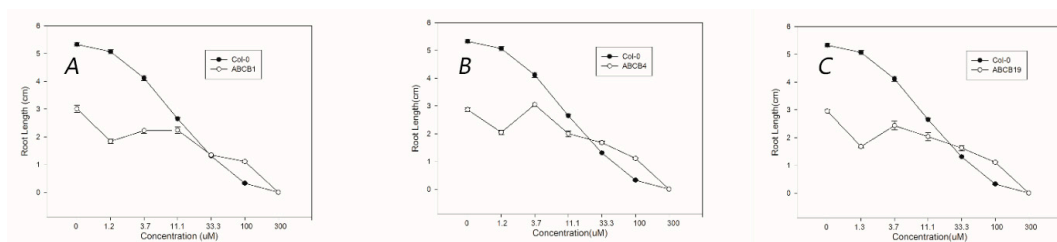


Figure 8. Root length of 3 biotypes at 7 days after treatment with 0 μM , 1.3 μM , 3.7 μM , 11.1 μM , 33.3 μM , 100 μM and 300 μM quinclorac. (A–C) represent the comparison of root length between *AtABCB1*, *AtABCB4*, *AtABCB19* and the parent line. Data are the mean values of at least 10 biological replicates. The standard errors of the means are described by vertical bars.

Table 4. The IC₅₀ were measured after treatment with quinclorac in the parent line and mutants.

Herbicide	Biotypes	IC ₅₀ μM	Regression Equation	Correlation Coefficient	Mutant IC ₅₀ /Parent IC ₅₀	Confidence Intervals
Quinclorac	Col-0	11.77	Y = 2.46x + 2.63		1	
	AtABCB1	10.61	Y = 0.32x + 4.67	0.99	0.90	0.64~1.25
	AtABCB4	49.91 *	Y = 0.84x + 3.57	0.99	4.24	3.14~5.71
	AtABCB19	44.03	Y = 0.86x + 3.58	0.99	3.74	3.31~4.22

Note: *, the IC₅₀ of mutants are significant higher compared with Col-0.

4. Conclusions

Our research explored a new mechanism of resistance to quinclorac. Quinclorac and NPA have the same inhibition phenotype on the root system of the seedlings of *E. crus-galli* var. *zelayensis*, which indicates that quinclorac may have the same mode of action as NPA. It is reported that AtABCB4 functions in the basipetal redirection of auxin from the root tip, and AtABCB1 [18] and AtABCB19 mediate auxin efflux [19]. In the susceptible population, the expression of *EcABCB4* (auxin-input) increased, and the expression of *EcABCB1* (auxin-output) and *EcABCB19* (basic transport) decreased after treatment with quinclorac, resulting in the accumulation of IAA at the root tip. Accumulation of IAA could stimulate the ethylene biosynthesis via increasing *1-Aminocyclopropane-1-Carboxylic Acid Synthase* (ACS) transcription [41]. Ethylene can inhibit photosynthesis, produce H₂O₂ and reactive oxygen species and lead to plant death. In the resistant population, the expression of *EcABCB1* and *EcABCB19* increased after treatment with quinclorac. At the same time, the expression of *EcABCB4* in resistance populations was lower than the susceptible, which could keep the normal concentration gradient of IAA, not stimulate the ethylene biosynthesis and yield quinclorac-resistant phenotypes.

Author Contributions: Y.S. performed root length and ELISA experiments; Y.Q., Y.G. (Yongli Guo) and X.L. were involved screening mutant, q-PCR and data analysis; J.L. supervised the project; Y.Q. wrote the manuscript with contributions from all authors; Y.G. (Yuan Gao) helped review; J.L. and L.D. were responsible for funding acquisition. All authors have read and agreed to the published version of the manuscript.

Funding: This research was funded by the National Key Research and Development Program of China (2021YFD1700100).

Data Availability Statement: This article contains all data.

Conflicts of Interest: The authors declare no conflict of interest.

References

- Xu, J.; Lv, B.; Wang, Q.; Li, J.; Dong, L. A resistance mechanism dependent upon the inhibition of ethylene biosynthesis. *Pest Manag. Sci.* **2013**, *69*, 1407–1414. [CrossRef]
- Grossmann, K. Quinclorac belongs to a new class of highly selective auxin herbicides. *Weed Sci.* **1998**, *46*, 707–716. [CrossRef]
- Grossmann, K. Auxin herbicides: Current status of mechanism and mode of action. *Pest Manag. Sci. Former. Pestic. Sci.* **2010**, *66*, 113–120. [CrossRef]
- Gao, Y.; Li, J.; Pan, X.; Liu, D.; Napier, R.; Dong, L. Quinclorac resistance induced by the suppression of the expression of 1-aminocyclopropane-1-carboxylic acid (ACC) synthase and ACC oxidase genes in *Echinochloa crus-galli* var. *zelayensis*. *Pestic. Biochem. Physiol.* **2018**, *146*, 25–32. [CrossRef] [PubMed]
- Grossmann, K.; Schmülling, T. The effects of the herbicide quinclorac on shoot growth in tomato is alleviated by inhibitors of ethylene biosynthesis and by the presence of an antisense construct to the 1-aminocyclopropane-1-carboxylic acid (ACC) synthase gene in transgenic plants. *Plant Growth Regul.* **1995**, *16*, 183–188. [CrossRef]
- Hall, J.C.; Bassi, P.K.; Spencer, M.S.; Vanden Born, W.H. An evaluation of the role of ethylene in herbicidal injury induced by picloram or clopyralid in rapeseed and sunflower plants. *Plant Physiol.* **1985**, *79*, 18–23. [CrossRef]
- Stepanova, A.N.; Yun, J.; Likhacheva, A.V.; Alonso, J.M. Multilevel interactions between ethylene and auxin in Arabidopsis roots. *Plant Cell* **2007**, *19*, 2169–2185. [CrossRef]
- Swarup, R.; Bennett, M. Auxin transport: The fountain of life in plants? *Dev. Cell* **2003**, *5*, 824–826.

9. Sánchez-Fernández, R.; Davies, T.G.E.; Coleman, J.O.; Rea, P.A. The Arabidopsis thaliana ABC protein superfamily, a complete inventory. *J. Biol. Chem.* **2001**, *276*, 30231–30244. [[CrossRef](#)]
10. Martinoia, E.; Klein, M.; Geisler, M.; Bovet, L.; Forestier, C.; Kolukisaoglu, U.; Müller-Röber, B.; Schulz, B. Multifunctionality of plant ABC transporters—More than just detoxifiers. *Planta* **2002**, *214*, 345–355. [[CrossRef](#)]
11. Petrusek, J.; Friml, J. Auxin transport routes in plant development. *Development* **2009**, *136*, 2675–2688. [[CrossRef](#)] [[PubMed](#)]
12. Bailly, A.; Yang, H.; Martinoia, E.; Geisler, M.; Murphy, A.S. Plant lessons: Exploring ABCB functionality through structural modeling. *Front. Plant Sci.* **2012**, *2*, 108. [[CrossRef](#)] [[PubMed](#)]
13. Noh, B.; Murphy, A.S.; Spalding, E.P. Multidrug resistance—Like genes of Arabidopsis required for auxin transport and auxin-mediated development. *Plant Cell* **2001**, *13*, 2441–2454. [[PubMed](#)]
14. Murphy, A.S.; Hoogner, K.R.; Peer, W.A.; Taiz, L. Identification, purification, and molecular cloning of N-1-naphthylphthalamic acid-binding plasma membrane-associated aminopeptidases from Arabidopsis. *Plant Physiol.* **2002**, *128*, 935–950. [[CrossRef](#)] [[PubMed](#)]
15. Geisler, M.; Kolukisaoglu, H.U.; Bouchard, R.; Billion, K.; Berger, J.; Saal, B.; Frangne, N.; Koncz-Kálmán, Z.; Koncz, C.; Dudler, R.; et al. TWISTED DWARF1, a unique plasma membrane-anchored immunophilin-like protein, interacts with Arabidopsis multidrug resistance-like transporters AtPGP1 and AtPGP19. *Mol. Biol. Cell* **2003**, *14*, 4238–4249. [[CrossRef](#)]
16. Terasaka, K.; Blakeslee, J.J.; Titapiwatanakun, B.; Peer, W.A.; Bandyopadhyay, A.; Makam, S.N.; Lee, O.R.; Richards, E.L.; Murphy, A.S.; Sato, F.; et al. PGP4, an ATP binding cassette P-glycoprotein, catalyzes auxin transport in Arabidopsis thaliana roots. *Plant Cell* **2005**, *17*, 2922–2939. [[CrossRef](#)]
17. Kamimoto, Y.; Terasaka, K.; Hamamoto, M.; Takanashi, K.; Fukuda, S.; Shitan, N.; Sugiyama, A.; Suzuki, H.; Shibata, D.; Wang, B.; et al. Arabidopsis ABCB21 is a facultative auxin importer/exporter regulated by cytoplasmic auxin concentration. *Plant Cell Physiol.* **2012**, *53*, 2090–2100. [[CrossRef](#)]
18. Geisler, M.; Blakeslee, J.J.; Bouchard, R.; Lee, O.R.; Vincenzetti, V.; Bandyopadhyay, A.; Titapiwatanakun, B.; Peer, W.A.; Bailly, A.; Richards, E.L.; et al. Cellular efflux of auxin catalyzed by the Arabidopsis MDR/PGP transporter AtPGP1. *Plant J.* **2005**, *44*, 179–194. [[CrossRef](#)]
19. Yang, H.; Murphy, A.S. Functional expression and characterization of Arabidopsis ABCB, AUX 1 and PIN auxin transporters in *Schizosaccharomyces pombe*. *Plant J.* **2009**, *59*, 179–191. [[CrossRef](#)]
20. Xu, Y.X.; Liu, Y.; Chen, S.T.; Li, X.Q.; Xu, L.G.; Qi, Y.H.; Jiang, D.A.; Jin, S.H. The B subfamily of plant ATP binding cassette transporters and their roles in auxin transport. *Biol. Plant.* **2014**, *58*, 401–410. [[CrossRef](#)]
21. Klein, M.; Geisler, M.; Suh, S.J.; Kolukisaoglu, H.; Azevedo, L.; Plaza, S.; Curtis, M.D.; Richter, A.; Weder, B.; Schulz, B.; et al. Disruption of AtMRP4, a guard cell plasma membrane ABCC-type ABC transporter, leads to deregulation of stomatal opening and increased drought susceptibility. *Plant J.* **2004**, *39*, 219–236. [[CrossRef](#)] [[PubMed](#)]
22. Lee, M.; Lee, K.; Lee, J.; Noh, E.W.; Lee, Y. AtPDR12 contributes to lead resistance in Arabidopsis. *Plant Physiol.* **2005**, *138*, 827–836. [[CrossRef](#)] [[PubMed](#)]
23. Rea, P.A. Plant ATP-binding cassette transporters. *Annu. Rev. Plant Biol.* **2007**, *58*, 347–375. [[CrossRef](#)] [[PubMed](#)]
24. Crouzet, J.; Roland, J.; Peeters, E.; Trombik, T.; Ducos, E.; Nader, J.; Boutry, M. NtPDR1, a plasma membrane ABC transporter from *Nicotiana tabacum*, is involved in diterpene transport. *Plant Mol. Biol.* **2013**, *82*, 181–192. [[CrossRef](#)] [[PubMed](#)]
25. Le Hir, R.; Sorin, C.; Chakraborti, D.; Moritz, T.; Schaller, H.; Tellier, F.; Robert, S.; Morin, H.; Bako, L.; Bellini, C. ABCG 9, ABCG 11 and ABCG 14 ABC transporters are required for vascular development in *A. rabidopsis*. *Plant J.* **2013**, *76*, 811–824. [[CrossRef](#)] [[PubMed](#)]
26. Shitan, N.; Dalmás, F.; Dan, K.; Kato, N.; Ueda, K.; Sato, F.; Forestier, C.; Yazaki, K. Characterization of *Coptis japonica* CjABCB2, an ATP-binding cassette protein involved in alkaloid transport. *Phytochemistry* **2013**, *91*, 109–116. [[CrossRef](#)]
27. Zhang, L.; Lu, X.; Shen, Q.; Chen, Y.; Wang, T.; Zhang, F.; Wu, S.; Jiang, W.; Liu, P.; Zhang, L.; et al. Identification of putative *Artemisia annua* ABCG transporter unigenes related to artemisinin yield following expression analysis in different plant tissues and in response to methyl jasmonate and abscisic acid treatments. *Plant Mol. Biol. Report.* **2012**, *30*, 838–847. [[CrossRef](#)]
28. Wilkens, S. Structure and mechanism of ABC transporters. *F1000prime Rep.* **2015**, *7*, 14. [[CrossRef](#)]
29. Goggin, D.E.; Cawthray, G.R.; Powles, S.B. 2,4-D resistance in wild radish: Reduced herbicide translocation via inhibition of cellular transport. *J. Exp. Bot.* **2016**, *67*, 3223–3235. [[CrossRef](#)]
30. Busi, R.; Goggin, D.E.; Heap, I.M.; Horak, M.J.; Jugulam, M.; Masters, R.A.; Napier, R.M.; Riar, D.S.; Satchivi, N.M.; Torra, J.; et al. Weed resistance to synthetic auxin herbicides. *Pest Manag. Sci.* **2018**, *74*, 2265–2276. [[CrossRef](#)]
31. Sunohara, Y.; Shirai, S.; Yamazaki, H.; Matsumoto, H. Involvement of antioxidant capacity in quinclorac tolerance in *Eleusine indica*. *Environ. Exp. Bot.* **2011**, *74*, 74–81. [[CrossRef](#)]
32. Tang, Q.Y.; Zhang, C.X. Data Processing System (DPS) software with experimental design, statistical analysis and data mining developed for use in entomological research. *Insect Sci.* **2013**, *20*, 254–260. [[CrossRef](#)] [[PubMed](#)]
33. Grossmann, K.; Kwiatkowski, J. Selective induction of ethylene and cyanide biosynthesis appears to be involved in the selectivity of the herbicide quinclorac between rice and barnyardgrass. *J. Plant Physiol.* **1993**, *142*, 457–466. [[CrossRef](#)]
34. Grossmann, K.; Scheltrup, F. Selective induction of 1-aminocyclopropane-1-carboxylic acid (ACC) synthase activity is involved in the selectivity of the auxin herbicide quinclorac between barnyard grass and rice. *Pestic. Biochem. Physiol.* **1997**, *58*, 145–153. [[CrossRef](#)]

35. Hansen, H.; Grossmann, K. Auxin-induced ethylene triggers abscisic acid biosynthesis and growth inhibition. *Plant Physiol.* **2000**, *124*, 1437–1448. [[CrossRef](#)]
36. Abdallah, I.; Fischer, A.J.; Elmore, C.L.; Saltveit, M.E.; Zaki, M. Mechanism of resistance to quinclorac in smooth crabgrass (*Digitaria ischaemum*). *Pestic. Biochem. Physiol.* **2006**, *84*, 38–48. [[CrossRef](#)]
37. Yang, X.; Han, H.; Cao, J.; Li, Y.; Yu, Q.; Powles, S.B. Exploring quinclorac resistance mechanisms in *Echinochloa crus-gavonis* from China. *Pest Manag. Sci.* **2021**, *77*, 194–201. [[CrossRef](#)]
38. Ljung, K.; Hull, A.K.; Celenza, J.; Yamada, M.; Estelle, M.; Normanly, J.; Sandberg, G. Sites and regulation of auxin biosynthesis in Arabidopsis roots. *Plant Cell* **2005**, *17*, 1090–1104. [[CrossRef](#)]
39. Mravec, J.; Kubes, M.; Bielach, A.; Gaykova, V.; Petrasek, J.; Skúpa, P.; Chand, S.; Benková, E.; Zazimalova, E.; Friml, J. Interaction of PIN and PGP transport mechanisms in auxin distribution-dependent development. *Development* **2008**, *135*, 3345–3354. [[CrossRef](#)]
40. Wu, G.; Lewis, D.R.; Spalding, E.P. Mutations in Arabidopsis multidrug resistance-like ABC transporters separate the roles of acropetal and basipetal auxin transport in lateral root development. *Plant Cell* **2007**, *19*, 1826–1837. [[CrossRef](#)]
41. Tsuchisaka, A.; Theologis, A. Unique and overlapping expression patterns among the Arabidopsis 1-amino-cyclopropane-1-carboxylate synthase gene family members. *Plant Physiol.* **2004**, *136*, 2982–3000. [[CrossRef](#)] [[PubMed](#)]